J|A|C|S
ARTICLES
Published on Web 01/09/2003

Structure and Dynamics of Metal Ions in Solution: QM/MM Molecular Dynamics Simulations of Mn^{2+} and V^{2+}

Christian F. Schwenk, Hannes H. Loeffler, and Bernd M. Rode*

Contribution from the Department of Theoretical Chemistry Institute of General, Inorganic and Theoretical Chemistry, University of Innsbruck, Innrain 52a, A-6020 Innsbruck, Austria

Received September 25, 2002; E-mail: bernd.m.rode@uibk.ac.at

Abstract: Structural and dynamical properties of the transition metal ions V^{2+} and Mn^{2+} in aqueous solution, resulting from combined quantum mechanical (QM)/molecular mechanical (MM) molecular dynamics (MD) simulations have been compared. The necessity of polarization functions on the ligand's oxygen for a satisfactory description of such ions in aqueous solution is shown using V^{2+} as test case. Radial distribution functions, coordination number distributions, and several angle distributions were pursued for a detailed structural comparison of the first hydration shells. Dynamical properties, such as the librational and vibrational motions of water molecules were evaluated by means of velocity autocorrelation functions. Approximative normal coordinate analyses were employed to calculate the rotational frequencies and vibrational motions around the three principal axes. The very low exchange rates for the first shell water exchanges only allow an investigation of the water exchange processes in the second shell, which take place within the picosecond range.

I. Introduction

Ion hydration plays an outstanding role because of its importance for such diverse fields as physics, biology, and chemistry.[1−3] Consequently, computer simulations in general, and molecular dynamics (MD) simulations[4] in particular, are of increasing importance to reveal details of molecular motions as well as structural and microscopic properties of the solution which are difficult to measure experimentally. Very accurate theoretical data based on correlated ab initio calculations are available for small ion−water complexes,[5−7] but they cannot be considered as a model for ions in solution, as in the liquid state the larger number of ligands, the second shell and the surrounding bulk produce an entirely different environment for the ion. Experimental investigations have to use assumptions to overcome counterion effects, which are nearly always present, as most experiments need to be performed in rather concentrated solutions.[8] For example, the symmetric M−O stretching frequencies for aqueous solutions have been determined by Raman spectroscopy which requires very high concentrations for detection.[9]

Many experimental studies have been performed to determine vibrational frequencies of water molecules in ionic solutions. Systematic studies for a series of metal ions[10,11] indicated a red-shift of the O−H stretching frequency due to the interaction with the metal ion. This can be interpreted in terms of strengthened hydrogen bonds between water molecules of the first and second hydration sphere, as the metal ion enhances the hydrogen bond by polarizing the water molecules.

Molecular Dynamics (MD) and Monte Carlo (MC) simulations allow a direct investigation of the molecular behavior of hydrated metal ions. Theoretical data often rely on classical force fields, in which the potential functions describing the inter- and intramolecular interactions are constructed by fitting an analytical formula to experimental data or ab initio calculations, and the subsequent simulations often use the assumption of pairwise additivity. This means cutting the series for the total intermolecular interaction energy of a *n*-body system, consisting of pair-, three-body up to higher-body interactions after the first term. It is well-known that the pairwise additive assumption for interaction potentials is not sufficient to describe structural properties of metal ions and recently it has been shown that simple three-body corrections do not allow the reproduction of all structural and dynamical properties of ionic solutions either.[12] Correct first shell hydration numbers can be obtained employing empirically fitted polarizable water models (SPC/E, RPOL).[13−16]

(1) Richens, D. T. *The Chemistry of Aqua Ions: Synthesis, Structure and Reactivity: A Tour Through the Periodic Table of the Elements*, 1st edition; Wiley: New York, 1997.
(2) Clapham, D. E. *Cell* **1995**, *80*, 259−269.
(3) Chazin, W. J. *Nat. Struct. Biol* **1995**, *2*, 707−710.
(4) Allen, M. P.; Tildesley, D. J. *Computersimulation of Liquids*; Oxford Science Publications: Oxford University Press: Walton Street, Oxford OX2 6DP, 1990.
(5) Trachtman, M.; Markham, G. D.; Glusker, J. P.; George, P.; Bock, C. W. *Inorg. Chem.* **2001**, *40*, 4230−4241.
(6) Trachtman, M.; Markham, G. D.; Glusker, J. P.; George, P.; Bock, C. W. *Inorg. Chem.* **1998**, *37* (17), 4421−4431.
(7) Siegbahn, P. E. M. In *New Methods in Computational Quantum Mechanics*; Prigogine, I., Rice, S. A., Eds.; John Wiley & Sons: 1996; Vol. 93, pp 333−387.
(8) Marcus, Y. *Pure Appl. Chem.* **1987**, *59* (9), 1093−1101.
(9) Kanno, H. *J. Phys. Chem.* **1988**, *92*, 4232−4236.
(10) Bergström, P.-Å.; Lindgren, J. *Inorg. Chem.* **1992**, *31*, 1529−1533.
(11) Kristiansson, O.; Villepin, J.; Lindgren, J. *J. Phys. Chem.* **1988**, *92*, 2680−2685.
(12) Schwenk, C. F.; Loeffler, H. H.; Rode, B. M. *J. Chem. Phys.* **2001**, *115* (23), 10 808−10 813.
(13) Floris, F.; Persico, M.; Tani, A.; Tomasi, J. *Chem. Phys. Lett.* **1992**, *199* (6), 518−524.
(14) Floris, F.; Martinez, J. M.; Tomasi, J. *J. Chem. Phys.* **2002**, *116* (13), 5460−5470.

10.1021/ja0286831 CCC: $25.00

These models, besides providing only a rigid water structure and hence no possibility to calculate vibrational frequencies, do not guarantee the correct implementation of all polarization and charge-transfer effects as an ab intio framework. For the description of electrolyte solutions the inclusion of many-body effects is compulsory for obtaining correct results, as polarization and charge transfer cause strong cooperative effects,[17] often letting the assumption of pairwise additivity break down.

The requirement for a good model of the system is to reproduce a wide range of properties including structure, IR and Raman spectra, exchange rates, etc. Because fluid systems consisting of a huge number of atoms are too large to be directly studied by traditional ab initio calculations, one of the recent approaches is to combine quantum mechanical (QM) and molecular mechanical (MM) methods.[18−20] We have already made use of this QM/MM MD technique in several studies which reliably predicted structural behavior of various metal ions in water in accordance with experimental data.[12,21−24]

Hybrid QM/MM MD simulations which partition the system into two regions, in which interactions are calculated separately, offer a breakthrough for the inclusion of higher many-body interactions in condensed phase systems. Many-body effects are included into the force field as the forces acting on molecules in a relevant subsystem are calculated by solving the Schrödinger equation. The implicit electronic contributions as charge transfer and polarization in the force field play an important role to obtain accurate structural data for main group[21,12] as well as transition metal ions.[22,23]

In contrast to Monte Carlo (MC) simulations, MD simulations using a flexible water model allow the evaluation of molecular motions such as librations and vibrations, whose frequencies can be calculated from velocity autocorrelation functions (VACF). The intramolecular vibrational motions of the water molecule take place within the fs-time scale, and the rotational librations are of sub-ps order, in general.

In previous studies the structures of the hydrated metal complexes $[Mn(H_2O)_6]^{2+}$ and $[V(H_2O)_6]^{2+}$ have been discussed in terms of radial distribution functions, coordination numbers, and angular distribution functions.[23,26,25] In this work the librational and vibrational motions of first and second hydration shell water molecules and bulk are examined by means of QM/MM MD simulations. The quantum mechanical treatment of the ion and its first hydration shell allows an estimation of the ion−water vibrational frequencies using approximative normal-coordinate analysis.[27,28]

II. Details of Calculations

A. QM/MM MD Methodology. The QM/MM method partitions the total system into a quantum mechanical (QM) region and a region treated by molecular mechanics (MM). All particles within the zone of main interest, e.g., the first hydration shell of the ion, are treated by means of quantum mechanics. Ion−water interactions within the molecular mechanical (MM) region are calculated using classical potentials constructed from QM calculations. The accuracy of a QM/MM calculation depends not only on the chosen QM and MM methods, but also significantly on the coupling model. Therefore, in each simulation step an ab initio calculation was performed providing quantum mechanical forces to be incorporated into the total force of the system by the following formula[29,30]

$$F_{\mathrm{tot}} = F_{\mathrm{MM}}^{\mathrm{sys}} + (F_{\mathrm{QM}}^{\mathrm{QM}} - F_{\mathrm{QM}}^{\mathrm{MM}})*S(r) \qquad (1)$$

where F_{tot} is the total force of the system, $F_{\mathrm{MM}}^{\mathrm{sys}}$ is the MM force of the total system, $F_{\mathrm{QM}}^{\mathrm{QM}}$ is the QM force in the QM region, and $F_{\mathrm{QM}}^{\mathrm{MM}}$ is the MM force in the QM region. The function S (ST2 switch[31]) ensures smooth and continuous transition from QM to MM region.

The QM/MM MD program used in this work allows water molecules to leave and enter the QM region as needed to be able to fully describe the dynamics of the system. The radii of the QM regions were estimated according to the radial distribution functions (RDF) obtained by previous classical MD simulations including three-body corrections and were set to 4.0 Å for Mn^{2+} and V^{2+}. The smoothing function was applied over a span of 0.2 Å.

The simulations were carried out with the QM/MM MD software package developed at our department using the parallelized version of the TURBOMOLE program[32,33] for the calculation of the ab initio forces by the unrestricted Hartree−Fock formalism. The basis sets used were the relativistic compact effective potentials (RCEP) and double-ζ valence basis set developed by Stevens et al. for Mn^{2+},[34] and Dunning's DZP for oxygen[35,36] and DZ for hydrogen.[35,36] The Los Alamos ECP plus DZ basis set[37,25] was used for V^{2+}, and alternatively DZ and DZP basis sets for oxygen and DZ for hydrogen. The same basis sets had been used to construct the pair- and three-body potentials for ion−water interactions.

B. QM/MM MD Simulations including Three-Body Corrections. The QM/MM MD simulations were performed with the same simulation protocol as in previous works.[22,21−23,25,26] The investigated system contained 1 Mn^{2+} or 1 V^{2+} ion and 499 water molecules in a periodic cube of side length 24.7 Å. The simulations took place at a temperature of 298.16 K in a canonical *NVT* ensemble. The temperature was kept constant utilizing the Berendsen algorithm[38] with a relaxation time of 0.1 ps and the density was assumed to be 0.997 g/cm^3 which is the density of pure water at the simulation temperature. The reaction field procedure[39] was employed in all simulations to correct the cutoff of long-range interactions and a flexible model for water including

(15) Jalilehvand, F.; Spångberg, D.; Lindqvist-Reis, P.; Hermansson, K.; Persson, I.; Sandström, M. *J. Am. Chem. Soc.* **2001**, *123* (3), 431−441.
(16) Koneshan, S.; Rasaiah, J. C. *J. Chem. Phys.* **2001**, *114* (17), 7544−7555.
(17) Elrod, M. J.; Saykally, R. J. *Chem. Rev.* **1994**, *94* (7), 1975−1997.
(18) Bakowies, D.; Thiel, W. *J. Phys. Chem.* **1996**, *100* (25), 10 580−10 594.
(19) Gao, J. In *Reviews in Computational Chemistry*; Lipkowitz, K. B., Boyd, D. B., Eds.; VCH Publishers: New York, 1996; Vol. 7, Chapter 3, pp 119−185.
(20) Warshel, A.; Levitt, M. *J. Mol. Biol.* **1976**, *103*, 227−249.
(21) Loeffler, H. H.; Rode, B. M. *J. Chem. Phys.* **2002**, *117* (1), 110−117.
(22) Inada, Y.; Mohammed, A. M.; Loeffler, H. H.; Rode, B. M. *J. Phys. Chem. A* **2002**, *106* (29), 6783−6791.
(23) Yagüe, J. I.; Mohammed, A. M.; Loeffler, H.; Rode, B. M. *J. Phys. Chem. A* **2001**, *105* (32), 7646−7650.
(24) Tongraar, A.; Liedl, K. R.; Rode, B. M. *J. Phys. Chem. A* **1998**, *102* (50), 10340−10347.
(25) Loeffler, H. H.; Yagüe, J. I.; Rode, B. M. *Chem. Phys. Lett.* **2002**, *363*, 367−371.
(26) Loeffler, H. H.; Yagüe, J. I.; Rode, B. M. *J. Phys. Chem. A* **2002**, *106*, 9529−9532.
(27) Bopp, P. *Chem. Phys.* **1986**, *106*, 205−212.
(28) Spohr, E.; Pálinkás, G.; Heinzinger, K.; Bopp, P.; Probst, M. M. *J. Phys. Chem.* **1988**, *92* (23), 6754−6761.
(29) Maseras, F.; Morokuma, K. *J. Comput. Chem.* **1995**, *16* (9), 1170−1179.
(30) Maseras, F. *Chem. Commun.* **2000**, *25*, 1821−1827.
(31) Stillinger, F. H.; Rahman, A. *J. Chem. Phys.* **1974**, *60* (4), 1545−1557.
(32) Ahlrichs, R.; von Arnim, M. In *Methods and Techniques in Computational Chemistry: METECC-95*; Clementi, E., Corongiu, G., Eds.; STEF: Cagliari, 1995; Chapter 13, pp 509−554.
(33) Ahlrichs, R.; Elliott, S. D.; Huniar, U. *Ber. Bunsen. Phys. Chem.* **1998**, *102* (6), 795−804.
(34) Stevens, W. J.; Krauss, M.; Basch, H.; Jasien, P. G. *Can. J. Chem.* **1992**, *70*, 612−630.
(35) Dunning, T. H., Jr. *J. Chem. Phys.* **1989**, *90* (2), 1007−1023.
(36) Dunning, T. H., Jr.; Hay, P. J. In *Modern Theoretical Chemistry: Methods of Electronic Structure Theory*; Schaefer, H. F., III, Ed.; Plenum Press: New York, 1977; Volume 3.
(37) Wadt, W. R.; Hay, P. J. *J. Chem. Phys.* **1985**, *82*, 284−298.
(38) Berendsen, H. J. C.; Grigera, J. R.; Straatsma, T. P. *J. Phys. Chem.* **1987**, *91* (24), 6269−6271.
(39) Adams, D. J.; Adams, E. M.; Hills, G. J. *Mol. Phys.* **1979**, *38* (2), 387−400.

intermolecular (CF2 model[40]) and intramolecular potentials[41] was employed (BJH water model). Because the BJH water model allows explicit hydrogen movement, a time step of 0.2 fs was chosen. The Newtonian equations of motion were treated by a general predictor-corrector algorithm. The cutoff was set to half the box length (12.35 Å).

The detailed description of the generation of the classical pair and three-body potentials has already been presented elsewhere.[22,25,42] To construct the ion−water pair potential function, Hartree−Fock energies (basis sets as above) were fitted with the Levenberg−Marquardt algorithm to the analytical formula

$$\Delta E_{2bd} = \sum_{i=1}^{3} \frac{A_{ic}}{r_{ic}^{a}} + \frac{B_{ic}}{r_{ic}^{b}} + \frac{C_{ic}}{r_{ic}^{c}} + \frac{D_{ic}}{r_{ic}^{d}} + \frac{q_i q_c}{r_{ic}} \tag{2}$$

where A, B, C, and D are the fitting parameters and the subscripts i and c indicate the ith atom of a water molecule and Mn^{2+} or V^{2+} ion, respectively. The three-body correction function was constructed by fitting energies from water−ion−water configurations to a function of the form

$$\Delta E_{3bd}^{corr} = A \exp(-B\, r_{12}) \exp(-B\, r_{13}) \exp(-C\, r_{23}) [(r_{limit} - r_{12})^2 (r_{limit} - r_{13})^2] \tag{3}$$

with the parameters A, B, and C. r_{limit} is a cutoff limit (set to 6.0 Å) up to which the three-body corrections are evaluated. The terms in square brackets ensure a smooth approach to zero for energies and forces at this limit.

Three different QM/MM MD simulations were carried out for Mn^{2+} and V^{2+}, testing the influence of a polarization function on oxygen of water by comparing the results of V^{2+} simulations using DZ and DZP basis sets for water. For Mn^{2+} the system was equilibrated for 4.6 ps taking the starting configuration from a previous classical MD pair potential simulation, collecting statistical data from further 20.0 ps of simulation. The system containing V^{2+} and DZ water molecules was equilibrated for 5.0 ps with a starting configuration from a previous classical MD simulation, sampling data within another 15.7 ps. Starting configurations for the simulation of V^{2+} with DZP water molecules were taken from the QM/MM MD simulation with DZ basis set for water and equilibrated for 2 ps. Statistical data were collected for further 10 ps.

C. Velocity Autocorrelation Functions. MD simulations (in contrast to Monte Carlo simulations) offer the possibility to investigate dynamical properties. The evaluation of velocity autocorrelation functions (VACFs) and their Fourier transformed power spectra provide essential information about hydrated ions.[4] The power spectra were obtained by cosine transformations.

The VACFs of oxygens and hydrogens contain all necessary information to analyze vibrational and librational frequencies of the hydrated ions. As the total spectrum can be obscured by overlapping bands, an approximative normal coordination analysis was utilized to obtain single bands.[27,28] The velocities of the hydrogens are projected onto the unit vector parallel to the corresponding O−H bond, perpendicular to the water plane; after subtracting the center of mass velocity of the water molecule, the normal coordinates of the system are obtained. In this way six projections (Q_1, Q_2, Q_3, R_x, R_y, R_z) are defined to describe the symmetric stretching, bending and asymmetric stretching vibration, and rotations around the three principal axes of the water molecule, respectively.[27,28] The instantaneous first shell oxygen velocities were projected in a similar way onto the ion−O vector to describe the corresponding stretching mode.

All frequencies of water molecules in the first hydration sphere of Mn^{2+} and V^{2+} determined by the QM/MM MD simulation were multiplied by scaling factors calculated for the corresponding DZ and DZP basis set (Table 1), because all atomic motions of these water molecules are generated according to the quantum theory-based forces calculated by the analytical gradient of the SCF wave functions. It is unclear, however, if the same scaling factor can be used uniformly over the whole frequency spectrum, because for instance no experimental data for librations exist.

The resulting scaling factors of 0.91 for DZ and 0.89 DZP are in agreement with the published standard scaling factor of 0.89 for a similar basis set.[44,45] The different scaling factors summarized in Table 1 for Q_1, Q_2, and Q_3 have been obtained from experimental and theoretical gas-phase frequencies for water. In the DZP case the three values are very similar (0.89) in contrast to the DZ values, which exhibit larger deviations from the average value of 0.91.

D. Mean Residence Times and Reorientational Times. To understand the dynamics of hydrated metal ions, it is important to have detailed information about the time water molecules stay in the hydration shell of the ion. In our case mean residence times (MRTs) have been calculated as proposed by Impey et al.[46] The algorithm makes use of the survival function

$$P_i(t) = \sum_{j=1}^{N_W} \frac{1}{N-t} \sum_{t_0=1}^{N-t} \prod_{k=t_0}^{t_0+t} A_{ij}(k) \tag{4}$$

described in detail by Garcia and Stiller,[47] where N_W is the number of water molecules, N the number of total time steps and A_{ij} is a binary sequence that answers yes or no (0 or 1) if a water molecule j lies within a defined region centered at site i at time step k. By definition $P_i(t = 0)$ is the average coordination number of the hydrate complex and $P_i(t)$ is the number of water molecules that are initially in the first hydration shell and still remain there after a time t.

Orientational dynamics may also be discussed in terms of reorientational time correlation functions (RTCFs)

$$C_{li}(t) = \langle P_l(\vec{u}_i(0)\vec{u}_i(t)) \rangle \tag{5}$$

where P_l is the Legendre polynomial of lth order and $\vec{u}_i$ is a unit vector along three principal axes i defined in a fixed coordinate frame as the rotations above.

As both MRT and RCTFs, are assumed to decay exponentially we decided to fit the RCTF to the simple formula

$$C_l(t) = a \exp(-t/\tau_1) \tag{6}$$

where a and τ_1 are the fitting parameters, and τ_1 is the corresponding relaxation time.

III. Results and Discussion

A. Structural Comparison of QM/MM-HF Simulations. In a previous paper,[26] the hydration structure of Mn^{2+} has been reported to be a hexa-coordinated complex, consistent with experimental results. The quantum mechanical treatment of the Mn^{2+} ion and its first hydration sphere makes it possible to reproduce the correct hydration structure, and is thus expected to reliably predict librational and vibrational frequencies in a

(40) Stillinger, F. H.; Rahman, A. *J. Chem. Phys.* **1978**, *68* (2), 666−670.
(41) Bopp, P.; Janscó, G.; Heinzinger, K. *Chem. Phys. Lett.* **1983**, *98* (2), 129−133.
(42) Yagüe, J. I.; Mohammed, A. M.; Loeffler, H. H.; Rode, B. M. *J. Mol. Struct. (THEOCHEM), 620(1)*, 15−20.
(43) Eisenberg, D.; Kauzmann, W. *The Structure and Properties of Water*; Oxford University Press: Oxford, 1969.
(44) Scott, A. P.; Radom, L. *J. Phys. Chem.* **1996**, *100*, 16 502−16 513.
(45) DeFrees, D. J.; McLean, A. D. *J. Chem. Phys.* **1985**, *82* (1), 333−341.
(46) Impey, R. W.; Madden, P. A.; McDonald, I. R. *J. Phys. Chem.* **1983**, *87* (25), 5071−5083.
(47) Garcıa, A. E.; Stiller, L. *J. Comput. Chem.* **1993**, *14* (11), 1396−1406.

dilute aqueous solution as well. The structural results of main interest for the Mn^{2+} ion are recalled in Table 2.

Two simulations with different basis sets for oxygen have been performed in the case of V^{2+}, using a DZ basis set[25] for the first and a DZP (present work) for the second run. The comparison of these results offers the possibility to estimate the influence of polarization functions at oxygen on the structural data, and to decide which basis set is sufficient to evaluate structural (and also dynamical) properties of main interest. The structural comparison of the QM/MM MD simulations for V^{2+} is summarized in Table 2.

The V−O RDFs are plotted in Figure 1 together with their running integration numbers. The first maxima are centered at 2.17 Å in the DZ and 2.23 Å in the DZP case and the second peak maxima corresponding to the second hydration shell are located at 4.3 Å (DZ) and 4.4 Å (DZP). As the basis set for water used in the QM region is the only difference between the two simulations, similar structures were expected for the outside MM region. In agreement with that the V−O RDFs for second shell and bulk are nearly identical, whereas the first DZP peak is smaller and broader. Accordingly the first DZ peak suggests a more rigid structure with lower radial flexibility of the water molecules. This can certainly be attributed to the absence of polarization functions on the oxygens. The first shell is well distinguishable from a second shell and the inter shell region is zero within a range of about 1 Å, indicating that no exchange occurred within the simulation time.

The first hydration shell of V^{2+} exhibits 100% of hexa-coordination. The second shell exhibits appreciable populations ranging from 14 to 18 in both cases and the nonzero RDF at the minimum after the second peak together with the low peak height indicate rapid exchanges with the bulk. The mean coordination numbers of the second shell are 16.4 (DZ) and 15.8 (DZP).

The main peaks of the O−V−O angular distribution functions (ADFs) are located at 90°/172° for DZ and 90°/173° for DZP, representing a nearly regular octahedron in both cases. The main peak of the DZ simulation is sharply pointed and narrow, in contrast to the smaller and broader peak of the DZP simulation, again indicating that the latter provides a more flexible first hydration shell.

The most probable θ angle (angle between ion−O vector and dipole vector) is found at 168° for DZ and 170° for DZP. The out-of-plane angle (angle between ion−O vector and water plane) is nearly zero in both cases (1° for DZ and −2° for DZP). Detailed analyses of the θ and out-of-plane angles show a strong difference in the shape of the obtained peaks. The very narrow and high first peak of the DZ simulation indicates low rotational flexibility of the coordinated water molecules in the $[V(H_2O)_6]^{2+}$ complex. The additional polarization function on oxygen induces a higher flexibility, resulting in smaller and broader peaks for θ and out-of-plane angles.

The water geometry in the first shell is listed in Table 2. For both basis sets, bond elongation and angle compression was observed with respect to gas-phase values.

The structural comparison of the two transition metal ions Mn^{2+} and V^{2+} using the values of Table 2 shows high similarity, especially in the metal−oxygen RDFs (Figure 2). The first peak of the Mn^{2+}−O RDF is smaller and broader than the V^{2+} peak located at a similar ion−oxygen distance. The second shell,

Table 1. Calculation of Scaling Factors for Bending and Stretching Modes (DZ and DZP basis set) Using the Experimental and Theoretical Gas Phase Values for Pure Water

	H_2O (DZ)	H_2O (DZP)	H_2O (exp)[a]	SF(DZ)[b]	SF(DZP)
Q_2 [cm^{-1}]	1711	1809	1595	0.932	0.882
Q_1 [cm^{-1}]	4029	4101	3657	0.908	0.892
Q_3 [cm^{-1}]	4205	4234	3756	0.893	0.887
ASF[c]				0.91	0.89

[a] Experimental frequencies in gas phase, ref 43. [b] Scaling Factor for vibrational frequencies. [c] Average scaling factor for vibrational frequencies.[44]

Table 2. Characteristic Structural Parameter for the First Hydration Shell of Mn^{2+} and V^{2+} (DZ and DZP basis set for oxygen)

	Mn^{2+} (DZP)[a]	V^{2+} (DZ)[b]	V^{2+} (DZP)
$r_{1,max}$ [Å][c]	2.25	2.17	2.23
$r_{2,max}$ [Å][d]	4.4	4.3	4.4
coordination number	6.0	6.0	6.0
mean O−M^{2+}−O angle [deg]	88/172	90/172	90/173
height[e]	3.9	5.4	4.5
WHH [deg][f]	20	14	17
mean θ angle [deg][g]	166	170	168
height	4.1	5.9	3.9
WHH [deg]	23	16	25
mean oop angle [deg][h]	6	1	−2
height	2.0	3.4	1.8
WHH [deg]	51	22	54
mean α(O−H−O) [deg]	107.0 (106.5)	110.6 (112.5)	105.3 (106.5)
mean d(O−H) [Å][i]	0.962 (0.947)	0.961 (0.951)	0.959 (0.947)

[a] QM/MM MD simulation at Hartree−Fock level using an additional three-body correction, see ref 26. [b] QM/MM MD simulation at Hartree−Fock level using an additional three-body correction, see ref 25. [c] First peak maximum of M^{2+}−O−RDF. [d] Second peak maximum of M^{2+}−O−RDF. [e] Peak height of main peak. [f] Peak width at half-height of main peak. [g] Angle between ion−O and dipole vector. [h] Angle between ion−O vector and water plane. [i] Optimized values for single water molecules with the corresponding DZ or DZP basis set in parentheses.

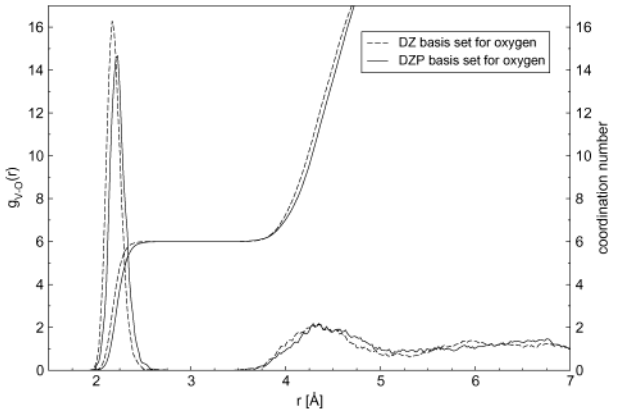

Figure 1. Comparison of the V−O radial distribution functions of the QM/MM simulations at HF-level using a DZ (broken line) and a DZP basis set (solid line) for oxygen.

however, is showing a well-defined peak for Mn^{2+} and V^{2+}. The first sphere depicts a more rigid structure for V^{2+} in contrast to the second one, which is better defined in the Mn−O RDF. Beyond the second hydration shell a random structure has been obtained in all cases.

The first hydration shell consists in both cases of six water molecules (100%) and the average coordination number of the second shell is nearly identical (15.9 for Mn^{2+} and 15.8 for V^{2+}). The angle distributions, as mean O−M^{2+}−O angle, mean θ angle and mean out-of-plane angle offer a rather similar picture of the two ions and the corresponding peaks exhibit a

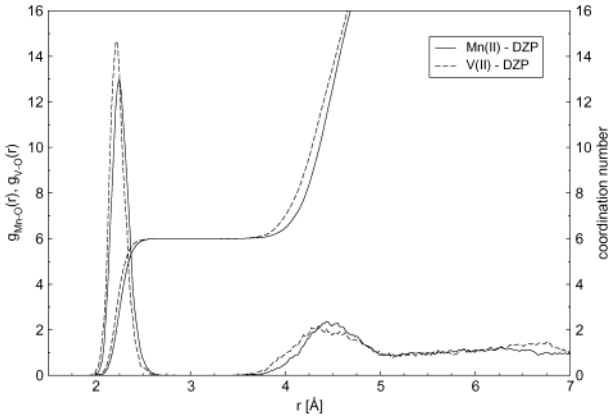

Figure 2. Comparison of the V−O and Mn−O radial distribution functions using DZP basis set for oxygen.

very similar shape. The influence of the two transition metal ions on the water geometry is rather similar showing nearly identical ion−O distances (0.959 Å for V^{2+} and 0.962 Å for Mn^{2+}) and a larger deviation of the DZP optimized water angle (106.5°) in the case of Mn^{2+}.

The QM/MM MD simulations of this work additionally give information about the hydration energy of the ions (ΔE_{hydr}) which can be compared to experimentally evaluated enthalpies of hydration. Some assumptions are necessary to estimate experimental data for single-ion hydration enthalpies, as the enthalpies measured for salts have to be assigned to separate anion and cation contributions.[48] The comparison of the resulting hydration energies for V^{2+} ($\Delta E_{hydr} = -560$ kcalmol^{-1}) and Mn^{2+} ($\Delta E_{hydr} = -550$ kcalmol^{-1}) with experimental values ($\Delta E_{hydr} = -404$ kcalmol^{-1} for V^{2+} and $\Delta E_{hydr} = -447$ kcalmol^{-1} for Mn^{2+} [48]) exhibits a deviation of 20 to 30%. Generally, literature values for the hydration energies show considerable variations and especially for V^{2+}, which is rather unstable in aqueous solutions, it is difficult to measure such data. The observed discrepancies are not very surprising, therefore, but the slightly weaker hydration energy found for Mn^{2+} seems consistent with other experimental observations of d^5 and d^{10} metal ions.[49]

B. Librational Motions and Residence Times. Figure 3 shows the librational motions together with intramolecular modes of first shell molecules for the three simulations. The normal mode approximation[27] works very well for all simulations as the single modes can be separated and coincide with the total spectrum. The frequencies corresponding to the power spectra of VACFs for the librational motions R_x, R_y, and R_z of the first hydration sphere of Mn^{2+} and V^{2+} are summarized in Table 3. In this work, we mainly concentrated on the QM treated first hydration shell, frequencies of the second shell or bulk are not included. The order $R_z < R_x < R_y$ found in this work is consistent with previous results.[26,53] The R_z wavenumbers of water molecules in the first shell of Mn^{2+} and V^{2+} are similar (DZ values for V^{2+} show the insufficiency of this basis set). Because the rotation about the dipole axis (R_z) is not energetically restricted by coordination to the metal ion, the R_z mode exhibits the smallest frequency of the librations. However, the motions leading to a change in dipole orientation, i.e., R_x and R_y, are strongly influenced by the interaction with the ion, and R_y is more strongly blue-shifted than R_x. Again, the smaller DZ basis set causes considerable deviations with values 10−20%

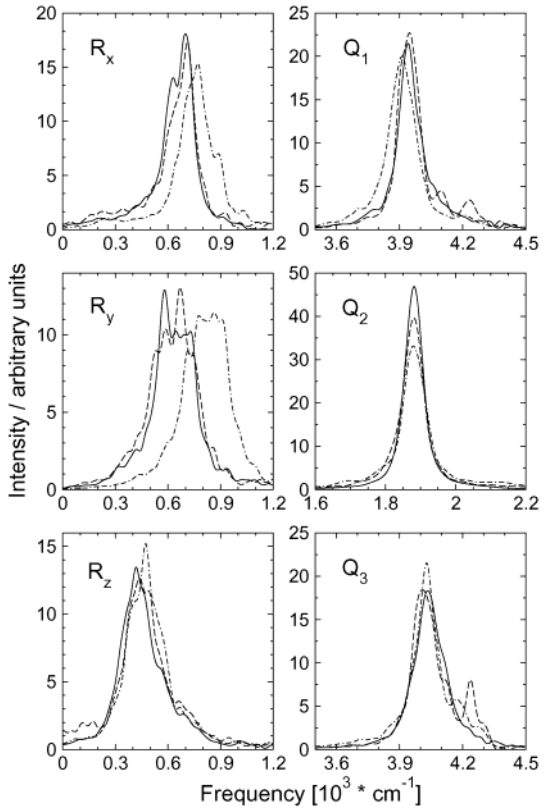

Figure 3. Power spectra of rotational modes R_x, R_y, R_z (left column) and vibrational modes Q_1, Q_2, Q_3 (right column) for water molecules in the first hydration sphere of Mn^{2+} (solid line), V^{2+} (DZP) (broken line), and V^{2+} (DZ) (dashdotted line).

Table 3. Vibrations, Librations, and Reorientation Times of First Shell Waters and Mean Residence Times of Second Shell Waters[j]

	Mn^{2+} (DZP)	V^{2+} (DZ)	V^{2+} (DZP)	H_2O (BJH)[a]	H_2O (exp)[b]	H_2O (gas)[c]
R_z[d]	418 (372)	472 (429)	438 (390)	415		
R_x	581 (517)	765 (696)	670 (596)	420		
R_y	700 (623)	863 (785)	712 (634)	540		
Q_2[e]	1882 (1675)	1882 (1713)	1881 (1674)	1698	1645	1610
Q_1	3941 (3507)	3912 (3560)	3947 (3513)	3455	3345	3650
Q_3	4035 (3591)	4029 (3666)	4010 (3569)	3552	3445	3768
Q_{iO}[f]	320 (285)	400 (364)	350 (312)			
τ_{1x}[g]	23 (31)	9.7 (21)	4.5	4.8	7.5[h]	
$\tau_1 y$	26	10	4.6	5.7		
$\tau_1 z$	47	63	136	6.6		
$\tau_2 x$	8.2	6.8	4.6	2.6		
$\tau_2 y$	10	7.7	4.9	3.3		
$\tau_2 z$	16	21	40	2.9		
τ_{MRT}[i]	7	25	4	3.0	2.5−10.0	

[a] Pure liquid simulation with the BJH water model.[41] [b] Experimental values for liquid water.[50] [c] Scaled HF values, see Table 1. [d] Librations about the three principal axes x, y, z. [e] Bending mode Q_2, symmetric stretch Q_1 and asymmetric stretch Q_3. [f] Stretching mode of the ion−O motion. [g] Reorientational times about the three principal axes x, y, z of first and second order; numbers in parentheses are exp data, see refs 51, 52. [h] Experimental reorientational correlation time of water.[51] [i] Mean residence times, eq 4, in the second hydration shell. [j] Numbers in parentheses are the wavenumbers scaled to allow direct comparison to experiment and classical simulations (Table 1). Frequencies in cm^{-1} and times in ps.

(48) Marcus, Y. *J. Chem. Soc., Faraday Trans.* **1987**, *83*, 339−349.
(49) Day, M. C.; Selbin, J. *Theoretical Inorganic Chemistry*; Reinhold Publisher Cooperation: New York, 1962.
(50) Murphy, W. F.; Bernstein, H. J. *J. Phys. Chem.* **1972**, *76* (8), 1147−1152.
(51) Ohtaki, H.; Radnai, T. *Chem. Rev.* **1993**, *93* (3), 1157−1204.
(52) Bloembergen, N.; Morgan, L. O. *J. Chem. Phys.* **1961**, *34*, 842−850.
(53) Bopp, P. *Pure Appl. Chem.* **1987**, *59* (9), 1071−1082.

higher than the ones obtained with the basis set containing polarization functions for oxygen. The comparison of scaled QM/MM wavenumbers with wavenumbers obtained from a classical simulation for Mn^{2+} [54] including three-body corrections shows deviations of 10−15% for the three librational motions, thus indicating the influence of higher *n*-body effects.

The R_z wavenumber is very similar for Mn^{2+} and V^{2+} using the DZP basis set for water but the DZ peak is shifted to higher frequencies in accordance with a more rigid structure. In agreement with structural data these facts maintain that first shell water molecules are mostly dipole oriented (*z* axis), i.e., rotation about this axis is not energetically restricted by the ion. However, the strongly inhibited rotations around the R_x and R_y axes keep the water molecules in the preferred orientation. The strongest inhibition of first shell water was obtained in the V^{2+} case with DZ basis set for water due to its missing polarization function for oxygen.

The QM/MM MD simulations make it possible to study the influence of cations (Mn^{2+} and V^{2+}) on rotational properties of the corresponding water molecules and on the rotational relaxation times obtained from eq 5. Table 3 lists values for RCTFs of first (τ_1) and second (τ_2) order, separately for the three principal axes as defined for the librations. For $l = 1$ these correlation functions are related to infrared line shapes and for $l = 2$ the correlation functions are related to Raman line shapes and NMR relaxation times.[51]

The RCTFs, depicted by six τ values, show very high numbers for the *z* axis (τ_{1z} and τ_{2z}) implying that the most probable movement is a rotation around the dipole axis. The RCTFs show strongly varying values and large differences between Mn^{2+} and V^{2+}. In the case of V^{2+} *x* and *y* values of the reorientational times (τ_{1x}, τ_{1y}, τ_{2x}, τ_{2y}) are smaller and *z* values turn out larger when using the DZP basis set for oxygen. The comparison of the two transition metals using the same DZP basis set for water exhibits a similar behavior with larger values for *x* and *y* and a smaller one for *z* in the case of Mn^{2+}. The vanadium ion (DZP) displays τ_{1x} and τ_{1y} values similar to pure BJH water and also τ_{2x}, τ_{2y} times very similar to the results obtained for pure BJH water. In contrast, the reorientational times along the *z*-axis are considerably higher. Our correlation times are similar to values obtained for Al^{3+}, Cr^{3+}, and Be^{2+} [55] and in good agreement with NMR measurements.[51]

The comparison of the QM/MM τ_1 results with classical data for reorientation times shows the importance of the inclusion of many-body terms. The classical simulation of Mn^{2+} [54] predicts the highest relaxation time for rotations around the *z* axis, in agreement with QM/MM results. The classical simulation strongly overestimates the stabilization around the *z* axis and consequently the rotation around the dipole axes, as for the QM/MM simulation the reorientational times about *x* and *y* axes are about half as big as the *z* value in contrast to the classical results being different by a factor of nearly 9.

C. Vibrational Motions. The vibrational frequencies from the power spectra of VACFs for Q_2, Q_1, and Q_3 are depicted in Figure 3 and summarized in Table 3. The scaled DZ V^{2+} frequencies are blue-shifted in comparison to the DZP V^{2+} values. The stretching modes Q_1 and Q_3 are red-shifted, the bending mode Q_2 blue-shifted relative to the gas phase indicating the polarization of first shell water molecules by the transition metal ion. Accordingly, the frequencies reflect bond angle compression and bond elongation of the H_2O (Table 2).

The frequency difference $\Delta\tilde{\nu}$ between Q_1 and Q_3 is about 80 wavenumbers for Mn^{2+} and 60 wavenumbers for V^{2+} similar to Ni^{2+} shifts ($\Delta\tilde{\nu} = 70$ cm^{-1}).[56] A comparison of the QM/MM wavenumbers with classical data including a three-body correction term in the case of Mn^{2+} [54] shows coincidence for the stretching mode Q_2. In contrast to that, the stretching modes Q_1 and Q_3 of the classical simulation are nearly 10% red-shifted, instead of the small blue-shift obtained by inclusion of *n*-body effects.

It is obvious from Table 3 that the BJH water model does not fully reproduce experimental data. The modes are blue shifted by about 50 cm^{-1} for Q_2 and about 100 cm^{-1} for Q_1 and Q_3. Thus, the frequencies obtained in this work are not to be considered on an absolute scale, but rather in terms of relative shifts. As such, they are reasonable and support all other structural analysis data. Scaling of the obtained frequencies even allows quantitative estimations, as the obtained bulk values are in good agreement with pure water results.

The scaled frequencies of the stretching modes of the ion−O motion may be separated as described above using the normal mode approximation. The obtained values, summarized in Table 3, were found to be 285 cm^{-1} for Mn^{2+} and 312 cm^{-1} for V^{2+} using the same DZP basis set for water. The V^{2+} simulation with DZ basis set for oxygen shows a high ion−O frequency (364 cm^{-1}) suggesting a lower flexibility of the hydrate complex in accordance with structural and librational results. The additional polarization function for oxygen has a strong influence on ion−O frequency increasing it by about 50 cm^{-1}. The force constant for Mn^{2+}−O ($k = 59$ Nm^{-1}) is clearly smaller than for V^{2+}−O ($k = 70$ Nm^{-1}) indicating a weaker ion−oxygen bond. This is in agreement with the slightly weaker hydration energy obtained for Mn^{2+} and the generally observed lesser ligand field stabilization of d^5 (and d^{10}) metal ions because of their specific electron density distributions.[49]

D. Water Exchange in the Second Hydration Sphere. The ligand exchange between coordination shells around metal ions is fundamental for the reactivity of these ions.[1] Water exchange at di- and trivalent transition metal ions has been the subject of extensive experimental studies.[57] In contrast to the fast exchanging alkali and alkaline earth ions which are very difficult to measure, experiments give easier access to exchange rates for the transition metal ions. As expected from experimental data, no water exchange between first and second hydration shell took place during simulation times of 20.0 ps for Mn^{2+}, 15.7 ps (DZ) and 10.0 ps (DZP) for V^{2+}. The experimental rate constant for water exchange of the first hydration spheres is 2.1×10^7 s^{-1} for Mn^{2+}.[57,58] No data are available for the very unstable V^{2+} ion. The expected exchange times are for sure larger than the longest QM/MM simulation times currently possible. Consequently, we mainly concentrated on the dynamics of the second hydration shell which is much more flexible. The detailed analysis of exchange processes between second shell and bulk

(54) Loeffler, H. H.; Rode, B. M. *J. Comput. Chem.*, submitted.
(55) Martınez, J. M.; Pappalardo, R. R.; Marcos, E. S. *J. Am. Chem. Soc.* **1999**, *121* (13), 3175−3184.
(56) Inada, Y.; Loeffler, H. H.; Rode, B. M. *Chem. Phys. Lett.* **2002**, *358*, 449−458.
(57) Helm, L.; Merbach, A. E. *Coord. Chem. Rev.* **1999**, *187*, 151−181.
(58) Lincoln, S. F.; Merbach, A. In *Advances in Inorganic Chemistry*; Academic Press: New Yrok, 1995; Vol. 42, pp 1−88.

supplied the mean residence times (τ_{MRT}) collected in Table 3 for the three simulations.

As a consequence of the rather short simulation times it is difficult to obtain accurate mean residence times, as the statistics is not very good. Nevertheless, QM/MM MD simulations allow a good estimation for these essential dynamical properties. The calculated values are 7 ps for Mn^{2+} and 4 ps for V^{2+} (DZP). The statistical problem becomes obvious as the survival function (4) approaches 2 (2 water molecules remain in the second hydration shell during the whole simulation) rather than the expected zero for long times.

The calculated τ_{MRT} values lead to about 60 exchanges during a simulation time of 20.0 ps for Mn^{2+}, and 50 exchanges in the case of DZP V^{2+} within 10 ps. The DZP results have been proven to be in agreement with the counted number of exchange processes during the simulation time. These values have been obtained by counting the water molecules crossing a border set to 5.3 Å (obtained from the $M^{2+}-O$ RDF; end of the peak of the second hydration shell) for more than 2 ps.

Ligand substitution mechanisms were classified by Langford and Gray by the symbols A (associative), D (dissociative), and I (interchange) for the different mechanisms proceeding via hepta- or pentacoordinated intermediates. There are two I mechanisms; I_a describes concerted reactions that have associative character and I_d represents concerted reactions that have dissociative character.

In our simulation of the liquid state the water exchange processes for Mn^{2+} mainly represent associative (A) mechanisms, but also interchange (I) and dissociative (D) mechanisms have been observed. The V^{2+} results show a large extent of dissociative (D) mechanisms in both cases (DZ and DZP).

IV. Summary and Conclusions

Our QM/MM MD approach proved suitable to take higher-body terms into account and to investigate the dynamical behavior of hydrate complexes, in addition to the structural data. Using two different double-ζ basis sets for water in the case of V^{2+} allowed to show the necessity of polarization functions on oxygen to correctly describe structural and dynamical data. Frequency shifts as obtained from power spectra maintain the notion of a dipole oriented first shell water molecule, thus confirming structural data. The QM/MM MD approach allows us to evaluate residence times and exchange processes between second shell and bulk and thus to estimate water exchange rates for the second hydration shell. This seems of particular importance, as the time scale of this exchange is in the picosecond range, which is hardly accessible by experimental methods. Consequently, QM/MM MD simulations have become a very reliable and sufficiently accurate tool to characterize ions in solution.

Acknowledgment. Financial support for this work from the Austrian Science Foundation (FWF) is gratefully acknowledged (project P13644-TPH).

JA0286831